JOURNAL OF BACTERIOLOGY, Mar. 1993, p. 1250–1256
0021-9193/93/051250-07$02.00/0
Copyright © 1993, American Society for Microbiology
Vol. 175, No. 5

Complete Structure of the Tyrosine-Linked Saccharide Moiety from the Surface Layer Glycoprotein of *Clostridium thermohydrosulfuricum* S102-70

RUDOLF CHRISTIAN,[1] GERHARD SCHULZ,[2] JUDITH SCHUSTER-KOLBE,[3] GÜNTER ALLMAIER,[4] ERICH R. SCHMID,[4] UWE B. SLEYTR,[3] AND PAUL MESSNER[3]*

Zentrum für Ultrastrukturforschung und Ludwig-Boltzmann-Institut für Molekulare Nanotechnologie, Universität für Bodenkultur, A-1180 Vienna,[3] Scientific Software Company, A-1140 Vienna,[1] Sandoz Forschungsinstitut Wien, A-1235 Vienna,[2] and Institut für Analytische Chemie, Universität Wien, A-1090 Vienna,[4] Austria

Received 16 October 1992/Accepted 16 December 1992

In this study, we have extended and completed a previous investigation (P. Messner, R. Christian, J. Kolbe, G. Schulz, and U. B. Sleytr, J. Bacteriol. 174:2236–2240, 1992) in which we demonstrated for the first time in prokaryotic organisms the presence of a novel O-glycosidic linkage via tyrosine. The surface layer glycoprotein of the eubacterium *Clostridium thermohydrosulfuricum* S102-70 is arranged in a hexagonal lattice, with center-to-center spacings of approximately 16.3 nm. Molecular weight determination by sodium dodecyl sulfate-polyacrylamide gel electrophoresis of both glycosylated and chemically deglycosylated surface layer glycoprotein showed values for the monomeric subunits of 94,000 and 87,500, respectively. Glycopeptide fractions obtained after exhaustive pronase digestion of purified, intact glycoprotein were isolated by reversed-phase liquid chromatography. One- and two-dimensional nuclear magnetic resonance studies, together with chemical analyses and plasma desorption time-of-flight mass spectrometry, were used to elucidate the structure of the hexasaccharide moiety linked by the novel O-glycosidic linkage to tyrosine. The combined evidence suggests the following structure: β-D-Gal*f*-(1→3)-α-D-Gal*p*-(1→2)-α-L-Rha*p*-(1→3)-α-D-Man*p*-(1→3)-α-L-Rha*p*-(1→3)-β-D-Glc*p*-(1→4)-L-Tyr.

Crystalline bacterial cell surface layers (S layers) constitute the outermost cell envelope of many prokaryotic cells (for reviews, see references 30, 40, and 41). About 15 years ago, the first report on a glycosylated S-layer protein of archaeobacteria was published (24). Since then, detailed structural, biosynthetic, and genetic studies have been performed on the cell surface glycoprotein of *Halobacterium salinarium* (*halobium*) (for a review, see reference 19). In eubacteria, however, covalently linked carbohydrate residues are mainly found in S layers in members of the family *Bacillaceae* (29). Prokaryotic glycoproteins can differ considerably from eukaryotic glycoproteins in their chemical structure and the composition of the linkage region (4).

Continuing our systematic survey of eubacterial S-layer glycoproteins, the present work described the ultrastructural and chemical characterization of the S-layer glycoprotein of *Clostridium thermohydrosulfuricum* S102-70. The complete structure of the glycan chain of a proteolytically derived glycopeptide fraction was derived from one- and two-dimensional nuclear magnetic resonance (NMR) spectroscopy measurements. Californium-252 plasma desorption mass spectrometry (^{252}Cf PD-MS) was used for the molecular weight determination and also allowed partial verification of the carbohydrate sequence determined.

In a previous report, we described the first characterization in prokaryotes of the O-glycosidic linkage between β-D-glucose and tyrosine (25). Since then, evidence that tyrosine also occurs in the S layer of *Acetogenium kivui* has been reported (33).

* Corresponding author.

MATERIALS AND METHODS

Organism and growth conditions. *C. thermohydrosulfuricum* S102-70 was obtained from F. Hollaus (Österreichisches Zuckerforschungs-Institut, Fuchsenbigl, Austria) and was grown at 60°C on S medium under anaerobic conditions in continuous culture as described before (25).

Electron microscopy. The S-layer lattice was characterized by freeze-etching of intact cells of *C. thermohydrosulfuricum*. The experiments were performed on a Balzers 400T freeze-etching unit (Balzers Union AG, Balzers, Liechtenstein) as described previously (26). Micrographs were recorded on a Philips EM 301 electron microscope at 80 kV.

Analytical methods. Carbohydrates and amino acids were analyzed as described before (25). Monosaccharides were determined after hydrolysis in 2 M trifluoroacetic acid (TFA) at 100°C for various times by high-performance anion-exchange chromatography (HPAEC) with pulsed amperometric detection on a Dionex series DX-300 high-pressure liquid chromatography (HPLC) system equipped with a CarboPac PA-1 column (Dionex Corp., Sunnyvale, Calif.). Amino acids were quantified on a Biotronic LC 3000 amino acid analyzer (Biotronic, Maintal, Germany), with norleucine used as an internal standard. All other analytical techniques followed described procedures (25). The optical rotation of the glycopeptide was determined with a Perkin Elmer model 243B polarimeter (Perkin Elmer, Norwalk, Conn.).

Preparation of the S-layer glycoprotein. Bacterial cells were broken and the intact S-layer glycoprotein was isolated from clean cell wall preparations by published methods (28). The purity of the preparations was checked by sodium dodecyl sulfate-polyacrylamide gel electrophoresis (SDS-PAGE) (26).

Deglycosylation of the S-layer glycoprotein. Intact S-layer

glycoprotein (5 mg) was suspended in a mixture of trifluoromethanesulfonic acid-anisole (2:1, 1 ml) and incubated at 0°C for 2 h (9). After extraction with diethyl ether containing 10% (vol/vol) hexane and washing with 95% ice-cold ethanol, the pellet was dissolved in 5 M guanidine hydrochloride and dialyzed against distilled water. The precipitate was lyophilized and subsequently analyzed by SDS-PAGE.

Isolation and purification of the S-layer glycopeptide. Pronase digestion of the intact S-layer glycoprotein and isolation of the glycopeptide fractions were done by previously described methods (25). Glycopeptide fraction III (GP III; 6 mg) was finally purified on a Beckman GOLD HPLC system (Beckman, San Ramon, Calif.) by reversed-phase liquid chromatography on an RP-18 column (Beckman; Ultrasphere octyldecyl silane; 5 μm, 4.6 by 150 mm). The material of interest was eluted with a linear gradient from 100% solvent A (0.1% TFA in water) to 10% solvent B (0.1% TFA in acetonitrile) over 30 min, with a flow rate of 1 ml/min. Detection was done at both 220 and 272 nm. Appropriate fractions were lyophilized and used for the structural analysis or stored at −20°C.

NMR spectroscopy. Spectra were recorded on a Bruker AMX-500 spectrometer (Bruker, Karlsruhe, Germany; 500.14 MHz, ^1H; 125.77 MHz, ^{13}C). The ^1H chemical shifts were determined for solutions in D_2O at 310 K and reported relative to an external reference of trimethylsilyl propionic acid in D_2O. The ^{13}C chemical shifts were measured at 298 K and reported relative to dioxane as an external reference at 67.40 ppm. ^1H-^{13}C correlation spectra and hetero-multiple-bond connectivity spectra (3) were recorded in the proton-detected mode at 310 K with a Bruker 5-mm inverse broadband probe with Bruker reversed electronics. Proton NMR shifts and couplings were refined by using the LAOCN5 program (Quantum Chemistry Program Exchange 458).

Mass spectrometry. The mass spectra of GP III were recorded on a Bio Ion 20K californium-252 plasma desorption time-of-flight spectrometer (Applied Biosystems, Foster City, Calif.) equipped with a 10-μCi ^{252}Cf source, using both the positive- and the negative-ion modes. The acceleration voltage applied was +17 and −15 kV for the molecular weight determination and +19 kV to determine positive-fragment ions with improved peak shapes. Time resolution was 1 ns per channel, and the spectra were accumulated for 2×10^6 to 2×10^7 fission events. Background was subtracted for all spectra shown in this study. The samples were dissolved in 5 μl of 0.1% TFA and applied to nitrocellulose-covered aluminized polyester foils by the spin-drying technique (32).

RESULTS

Characterization of S-layer glycoprotein and glycopeptide. Freeze-etching of intact cells of *C. thermohydrosulfuricum* S102-70 showed that the bacteria are completely covered by a hexagonally arranged S-layer lattice with a center-to-center spacing of the morphological units of approximately 16.3 nm (Fig. 1). Each morphological unit consists of six identical subunits with an apparent molecular weight of 94,000 on SDS-PAGE (not shown). Upon deglycosylation of the S-layer glycoprotein by trifluoromethanesulfonic acid treatment, the molecular weight of the individual subunits decreased slightly to approximately 87,500 (not shown). Chemical analysis of this material yielded a total of approximately 4.5% (wt/wt) carbohydrates, with 1.3% (wt/wt) rhamnose (25). Based on this amount of sugar, an average of four to five glycosylation sites per S-layer subunit was calculated.

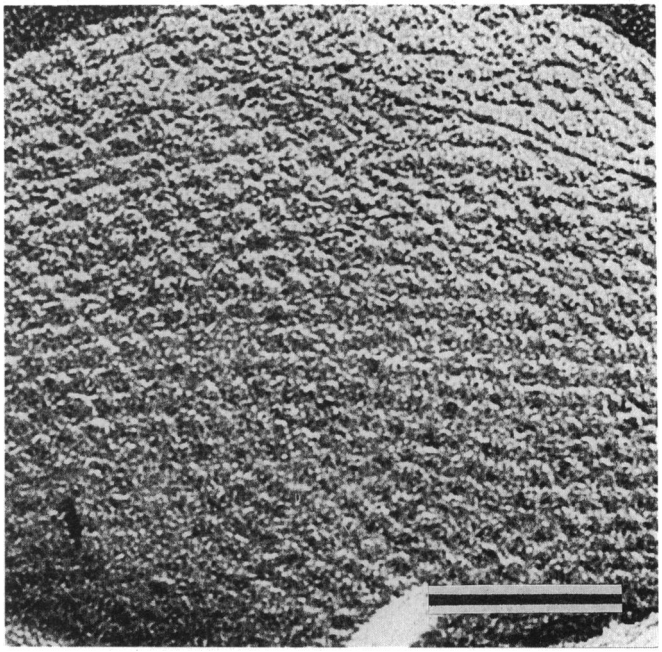

FIG. 1. Electron micrograph of a freeze-etched preparation of intact cells of *C. thermohydrosulfuricum* S102-70, showing the hexagonal S-layer lattice. Bar, 100 nm.

Since fraction GP III was obtained after pronase digestion and Bio-Gel P-4 chromatography (25), this material was subjected to reversed-phase HPLC (Fig. 2) to remove possible contaminants. No significant loss of carbohydrate-containing material was observed. The eluted specimen showed absorption at both 272 and 220 nm, indicating the presence of an aromatic compound. It eluted from the RP-18 column as a single, sharp peak and showed tyrosine as the only component in amino acid analysis. Monosaccharide

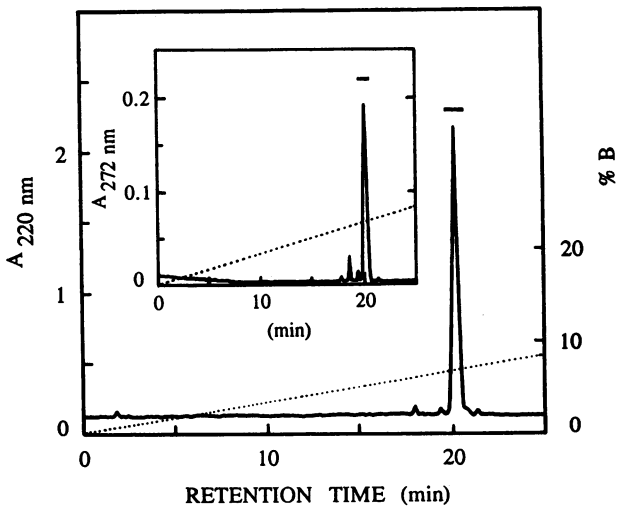

FIG. 2. Final purification of GP III by reversed-phase HPLC on an RP-18 column at 220 and 272 nm (inset). Material was eluted from the column with a linear gradient (···) from 100% solvent A (0.1% TFA in water) to 10% solvent B (0.1% TFA in acetonitrile) over 30 min, with a flow rate of 1 ml/min. Fractions were pooled as indicated by the bar.

TABLE 1. NMR chemical shifts and coupling constants of GP III from *C. thermohydrosulfuricum* S102-70 in D_2O

Assignment	Value[a] for residue (unit):						
	β-Gal*f* (A)	α-Gal*p* (B)	α-Rha*p* (C)	α-Man*p* (D)	α-Rha*p* (E)	β-Glc*p* (F)	Tyr
^1H							
H-1	5.249	5.121	5.150	5.113	5.239	5.146	
H-2	4.213	3.976	4.092	4.233	4.324	3.705	7.294
H-3	4.090	4.027	3.994	4.012	3.943	3.732	7.135
H-4	4.068	4.183	3.580	3.817	3.569	3.589	
H-5	3.854	4.305	4.026	3.980	4.095	3.654	
H-6a	3.721	3.746	1.318	3.901	1.301	3.948	
H-6b	3.672	3.746		3.823		3.773	
H-7a							3.252
H-7b							3.105
H-8							4.085
$J_{H,H}$							
1,2	1.9	4.1	1.9	2.0	2.0	8.0	
2,3	3.7	10.5	3.4	3.2	3.2	8.5	8.5
3,4	6.4	3.2	9.7	9.8	9.6	9.5	
4,5	4.4	1.0	9.7	9.9	9.8	10.1	
5,6a	4.5	6.1	6.3	2.2	6.4	1.8	
5,6b	7.2	6.1		5.7		5.6	
6a,6b	−11.7	−12.6		−12.3		−12.7	
7a,7b							−14.1
7a,8							4.5
7b,8							8.0
^{13}C							
C-1	109.97	98.61	94.97	97.11	101.82	100.90	130.69
C-2	82.38	68.25	77.28	67.53	67.28	74.41	131.69
C-3	77.71	77.84	70.59	76.32	75.34	82.93	117.99
C-4	83.67	70.09	72.84	65.71	71.16	68.80	156.92
C-5	71.64	71.68	70.00	73.60	69.85	77.02	
C-6	63.61	61.73	17.43	61.73	17.55	61.45	
C-7							35.76
C-8							56.94

[a] ^1H and ^{13}C shifts are given in ppm; $J_{H,H}$ coupling constants are given in Hz.

analysis by HPAEC yielded galactose, rhamnose, mannose, and glucose in a molar ratio of 2.0:2.1:1.0:1.0. The ratio of glucose to tyrosine was found to be 1:1. This material was then used in both the NMR and mass spectrometry experiments.

NMR measurements. The ^1H NMR spectrum of the isolated glycopeptide fraction recorded at 310 K showed signals of 51 protons (by integration). Four of them were recognized to belong to a *para*-substituted phenyl system (7.294 and 7.135 ppm). Six protons were identified as anomeric protons of carbohydrates (5.249, 5.239, 5.150, 5.146, 5.121, and 5.113 ppm), 33 protons were in the range of 3.6 to 4.3 ppm (sugar ring and side chain protons), two protons were recognized to belong to a $CH\text{-}CH_2$ system (3.105 and 3.252 ppm), and six protons of two methyl groups were found at 1.318 and 1.301 ppm. Since the proton signals of the individual sugar units overlapped heavily, selective decoupling and correlated spectroscopy and total correlated spectroscopy allowed only partial determination of proton-proton connectivities.

The ^{13}C NMR spectrum showed 41 signals for 44 carbons. In agreement with the proton spectrum, four signals at 118 to 157 ppm could be observed at the positions where the carbons of a *para*-substituted phenyl system should be expected. Six signals were in the range of 95 to 110 ppm, where anomeric carbons of pyranoid and furanoid carbohydrates reside. Four signals at 61.4 to 63.6 ppm indicated unsubstituted sugar side chain CH_2OH groups. Two signals at 17.4 and 17.5 ppm originated from 6-deoxy sugars, suggesting a sequence of six sugars not linked via side chains. Finally, although no signal of a carboxyl carbon could be observed, the signals at 35.8 and at 56.9 ppm, together with that of the phenyl ring, were in good agreement with expected values for tyrosine (44).

To get information about linkages between the individual sugar units and to obtain some proton-carbon connectivities suitable for assignment of proton shifts by means of proton-carbon correlated spectroscopy, a hetero-multiple-bond connectivity experiment (3) was performed. Except for the connectivity from H-1 of unit F (Table 1) to C-4 of tyrosine, all 2-, 3-, and 4-bond carbon-proton connectivities were observed. In addition, all signals where unit F protons are involved were weak. A possible explanation for the missing and weak signals of the unit F part is that either the carbon-proton couplings are small (3) or the intensities were low because of short relaxation times. The published shorter relaxation rates of phenolic glycosides (13) support the latter possibility.

The information obtained about the proton-carbon connectivities (e.g., H-1 of pyranoid rings to C-2, C-3, and C-5 as well as to the glycosidic bonded carbon; H-1 of furanoid rings to C-2, C-3, C-4, and the glycosidic bonded carbon; H-2 to C-1, C-3, C-4, and, if substituted, the corresponding anomeric carbon; up to H-6 to C-5 and C-4), in combination with carbon-proton correlations, was used together with the proton-proton connections obtained partly from correlated and total correlated spectroscopy. These data enabled us to sort the proton and carbon shifts into groups, A to F (Table 1). The proton shift positions now available allowed us to simulate the proton subspectra of the individual sugar subunits. Thus, the stereochemistry of individual sugar units B

TABLE 2. Observed and calculated ^{13}C shift differences between GP III and monosaccharides[a]

Linkage[b]	Stereochemistry[c]	Δ^{13}C shift (ppm)							
		C-1		C-2		C-3		C-4	
		Observed	Calculated (expected)	Observed	Calculated (expected)	Observed	Calculated (expected)	Observed	Calculated (expected)
A→B	$2a^1T_0(1a\rightarrow3e)^4C_12e4a$ [$\approx 2a^1C_4(1a\rightarrow3e)^4C_12e4a$]	1.07	1.2 (−3.8)	0.78	0.6 (−0.2)				
B→C	$2e^4C_1(1a\rightarrow2a)^1C_41a3e$	−1.52	−1.6 (1.5)	−0.77	−0.7 (−3.0)	7.55	8.1	0.04	−0.4
C→D	$2a^1C_4(1a\rightarrow3e)^4C_12a4e$	−6.77	−4.9 (−0.1)	6.38	6.8 (9.3)	−0.63	−0.6 (−0.4)	−0.07	0.0 (0.2)
D→E	$2a^4C_1(1a\rightarrow3e)^1C_42a4e$	−4.46	−3.7 (1.3)	−3.27	−3.3 (−0.2)	4.96	4.2 (7.3)	−1.87	−1.9 (−0.8)
E→F	$2a^1C_4(1a\rightarrow3e)^4C_12e4e$	0.08	0.2 (0.2)	−3.62	−3.8 (0.0)	4.12	3.8 (7.5)	−1.75	−1.8 (−0.7)
F→Tyr	$2e^4C_1(1e\rightarrow4)$Tyr	−3.04	−2.9 (−2.6)	0.49	0.5 (−1.4)	6.35	6.7 (6.5)	−1.68	−1.6 (0.4)

[a] The tabulated ^{13}C shift differences were obtained by subtracting the shift values of the corresponding methyl glycosides (β-Gal*f*-OMe and α-Rha*p*-OMe [12]; α-Gal*p*-OMe, β-Glc*p*-OMe, and α-Man*p*-OMe [34]) from the experimental values observed for GP III. The expected values for the opposite stereochemistry are given in parentheses. To predict the chemical shift differences, appropriate disaccharide models were used (5, 13, 14, 20, 21, 35). If no references for model compounds (glycosidation and substitution shifts) were available, average values were used (39).

[b] The unit for which the carbon shift differences were calculated is listed first.

[c] As an example, $2a^1C_4(1a\rightarrow3e)^4C_12e4a$ means that a pyranoside in the $^1C_4$ chair conformation (L-series) with both axial O-1 and axial O-2 is linked to an equatorial O-3 of a pyranoside in the $^4C_1$ chair conformation (D-series) with equatorial O-2 and axial O-4.

to F could be determined from proton-proton coupling constants. Unit B was identified as α-galactose, units C and E were identified as rhamnose, unit D was identified as mannose, and unit F was identified as β-glucose. Since in manno-systems, α and β H-1 protons have similar coupling constants to H-2, additional assessment criteria were necessary. Both rhamnoses (units C and E) could be assigned to the α-series, based on the proton shift values of H-3 and H-5, which were close to 4 ppm (18). Unit D was identified as α-mannose by using the carbon shift values of an α-Man*p*-(1→3)α-Rha*p* reference compound (7). The chemical shift value of the anomeric carbon of mannose differed by 0.06 ppm and the shift value of C-3 of the attached rhamnose by 0.09 ppm from the model compound. Finally, unit A was identified as β-galactofuranose, based on the significant C-1 to C-6 carbon shift values of β-galactofuranose, which compared well with those of the corresponding methyl glycoside (37).

Although no direct connection to C-4 of tyrosine could be measured for unit F, the linkage to the phenolic oxygen could be verified by using reference compounds. First, the carbon shift values observed for phenolic β-glycosides were significantly different from those of other glycosides (6). Second, taking into account the α-rhamnose substitution shift at C-3 of glucose (5), the carbon shift values fitted remarkably well to those observed for synthetic glycosyltyrosine (22).

Kochetkov et al. (17) have shown that the absolute configuration of carbohydrates can be determined relative to that of the glycosidic bonded sugar by using carbon shift values. The differences in the carbon shift values of carbons close to the glycosidic oxygen and those of monosaccharides are mainly determined by the ring conformation, $^4C_1$ or $^1C_4$, of both sugar units, the axial or equatorial orientation of O-1 and O-2 of the substituting sugar, and the oxygens vicinal to the glycosidic oxygen of the substituted sugar (Table 2). Thus, for β-D-galactofuranose in the $^1T_0$ conformation (43), which, in terms of the linkage region, behaves like an α-L-mannopyranose, no major differences were expected in comparison to the corresponding methyl glycoside if it is linked to O-4 of α-galactose (Table 2, A→B). Therefore, both galactoses belong to the same stereochemical series. For α-galactopyranose linked to C-2 of α-rhamnose (Table 2, B→C), an upfield shift was observed compared with the methyl glycoside. If both sugars belong to the same stereochemical series, a downfield shift on C-1 of galactose would be expected. For α-rhamnose linked to C-3 of mannose (Table 2, C→D), a large upfield shift was expected in comparison to the methyl glycoside. This was considered proof that both sugars belong to different stereochemical series. The upfield shift was further enhanced by the β-shift from substitution at C-2, which explained the unusual value of 95 ppm for the anomeric carbon of α-rhamnose. For α-mannose, if linked to C-3 of rhamnose (Table 2, D→E), a large C1 upfield shift was expected, and indeed observed, when it was compared with the corresponding methyl glycoside. Finally, for α-rhamnose-(1→3)-glucose linkages (Table 2, E→F), no major effects were expected at C-1 in either stereochemical combination. However, the β-shifts observed at C-2 and C-4 of glucose are different (5), verifying that units E and F belong to different stereochemical series.

Since ^{13}C NMR shift values reveal only the configurations of individual sugar subunits relative to connected ones (DDLDLD→Tyr or LLDLDL→Tyr), the assumed absolute configurations were verified by optical rotation measurement. As a proof of the anomeric configurations determined for the constituent sugars and L-tyrosine, the optical rotation of GP III was calculated by using Klyne's rule (16). The calculated value of $[\alpha]_D = 1.1°$ is close to $[\alpha]_D^{20} = -9.09°$ (c = 0.869, water), which was observed for the glycopeptide (Table 3). This result supports the initial assumption that galactose, glucose, and mannose were present in the D-form, whereas rhamnose and tyrosine were present in the L-form.

Finally, the proposed glycopeptide structure was verified by mass spectrometry. In the positive-ion mode (Fig. 3a), the cationized molecular ion $(M + Na)^+$ was observed at m/z 1,145.07 (calculated, 1,145.06). Additionally, an abundant $(M + 2Na - H)^+$ ion was detected at m/z 1,167.12 (calculated, 1,167.04). In the negative-ion mode (Fig. 3b), an intense deprotonated molecular ion was observed at m/z 1,121.08 (calculated, 1,121.06). The positive-ion mass spectrum exhibited an extensive series of useful fragment ions. These ions could be correlated with the sugar sequence determined. The most helpful fragment ions in terms of the monosaccharide sequence of GP III were two series of sodium-carrying fragments (series A and C, according to the nomenclature of Aduru and Chait [1]). Series A corresponded to sugar ring cleavage, with retention of HCO on

TABLE 3. Comparison of calculated and observed optical rotation of GP III from *C. thermohydrosulfuricum* S102-70 with that of model substances

Compound (reference)	Optical rotation (degrees)	
	$[\alpha]_D$	$[M]_D$[a]
Methyl-α-D-galactopyranoside (8)	196.1	380.8
Methyl-β-D-galactofuranoside (2)	−112.0	−217.5
Methyl-β-D-glucopyranoside (8)	−34.2	−66.4
Methyl-α-D-mannopyranoside (10)	79.2	153.8
Methyl-α-L-rhamnopyranoside (11)	−67.2	−119.7
L-Tyrosine (45)	−13.2	−23.9
GP III		
Calculated (16)	−1.1	−12.6
Observed	−9.1	−102.0

[a] Molecular rotation.

TABLE 4. Measured and calculated masses of fragment ions of GP III, obtained by ^{252}Cf PD-MS in the positive-ion mode at +19 kV

Ion[a]	m/z	
	Measured	Calculated
A_5	1,010.5	1,010.9
A_4	848.8	848.8
A_3	703.0	702.6
A_2	540.7	540.5
A_1	—[b]	394.3
C_5	964.5	964.9
C_4	802.3	802.8
C_3	655.8	656.6
C_2	494.4	494.5
C_1	—[b]	348.3

[a] $A_i = [M + Na + HCO - \{(6 - i)S + H\}]^+$ and $C_i = [M + Na - OH - \{6 - i)S + H\}^+$, where M is the average mass of the compound and S is the average mass of the individual sugar units (146.2 for rhamnose and 162.1 for galactose, glucose, and mannose). The nomenclature of the fragment ions corresponds to that of Aduru and Chait (1).

[b] The mass could not be detected unambiguously because of the low abundance of the fragment ions and/or interfer background ions.

the glycosidic oxygen of the charged, amino acid-containing fragment. Series C appeared to result from cleavage at the glycosidic oxygen, with retention of this oxygen on the charged fragment, transfer of a hydrogen atom to this fragment, and loss of water from the charged fragment. The observed and calculated *m/z* values of the fragments of each series are summarized in Table 4.

The combined chemical evidence and one- and two-dimensional NMR analyses permit the structure of the glycan to be established as a hexasaccharide linked by an O-glycosidic linkage to tyrosine: β-D-Gal*f*-(1→3)-α-D-Gal*p*-(1→2)-α-L-Rha*p*-(1→3)-α-D-Man*p*-(1→3)-α-L-Rha*p*-(1→3)-β-D-Glc*p*-(1→4)-L-Tyr.

DISCUSSION

We analyzed the S-layer lattice of *C. thermohydrosulfuricum* S102-70 by electron microscopy (Fig. 1). Each morphological unit of the hexagonal S-layer lattice consisted of six identical subunits with an apparent molecular weight of 94,000. Unlike all other S-layer glycoproteins investigated previously (29), only a minor shift in the molecular weight from 94,000 to 87,500 was observed after deglycosylation. This was a good indication that rather short glycan chains were present on the native S-layer glycoprotein and excluded the possibility of unspecific hydrolytic degradation during sample preparation. As calculated from the molecular weights, at least four tyrosine residues of the complete S-layer polypeptide backbone were assumed to become glycosylated per S-layer subunit. After isolation of the S-layer glycoprotein and exhaustive pronase digestion, the major degradation product (GP III [25]) was finally purified by HPLC for the NMR and mass spectrometry experiments.

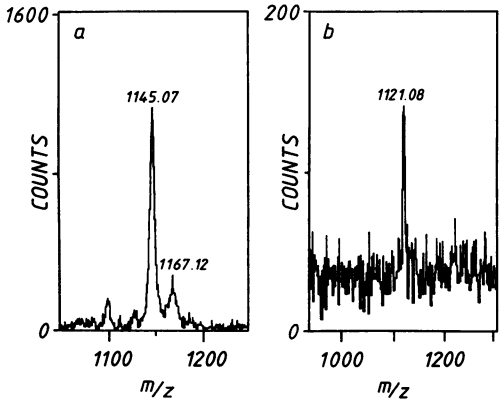

FIG. 3. (a) Positive-ion ^{252}Cf PD-MS of GP III, showing ions formed by single and double sodium ion attachment to the underivatized molecule at *m/z* 1,145.07 and *m/z* 1,167.12. (b) Negative-ion ^{252}Cf PD-MS of the same preparation, showing an ion formed by deprotonation of the underivatized molecule at *m/z* 1,121.08.

Analysis of this preparation by ^{1}H and ^{13}C NMR techniques showed the presence of a hexasaccharide moiety linked to tyrosine (Table 1). Usually, the glycan chains in glycosylated S layers consist of approximately 10 to 50 repeats (for a review, see reference 29). Interestingly, galactose was present in the hexasaccharide in both the furanosidic and pyranosidic forms. At the nonreducing end, the chain is terminated by galactofuranose. It could be that in this particular case, the galactofuranose has acted as a termination signal for chain elongation in the S-layer glycoprotein. The heterosaccharide is linked to the amino acid via an O-glycosidic linkage from β-D-glucose to the phenolic OH-group of tyrosine, which is novel in prokaryotes (25). The presence of the aromatic ring system caused some unusual downfield shifts (Table 1) on the β-glucose residue, indicating that H-1_F is in close vicinity to the phenylic ring system. In addition, the proton signals of the glucose residue were broadened at 298 K, indicating a restricted mobility of the glucose when linked to tyrosine.

The biological role of the carbohydrate chain might be to protect the protein against proteolytic attack. This assumption correlated well with previous difficulties in obtaining glycopeptide fraction GP III from the intact S-layer glycoprotein when pronase was used for the digestion (25). Obviously, steric hindrance due to spreading of the glycans over the protein surface is the reason for the hindered proteolytic degradation. Such phenomena were also described by Montreuil (31) for eukaryotic glycoproteins. The results of the structural analysis of GP III obtained by the NMR experiments were confirmed by ^{252}Cf PD-MS in both the positive- and negative-ion mode.

Nothing is yet known about the biological function(s) of the glycan portion in S-layer proteins (for reviews, see

references 29 and 30). From our screening of *Bacillaceae* species and lactobacilli, we can conclude that glycosylation of S-layer proteins is not a very frequent event (27). In this context, which type of selection pressure leads to this complex, energy-consuming modification of S-layer proteins is an important question. In speculations about the roles of the carbohydrates in S layers (29, 30), one should also take into account the possible global effect of the glycan chains on the stability of a protein. A recent comparison of nonglycosylated and glycosylated forms of RNase has demonstrated that the structure of the protein is essentially unaffected by glycosylation. Glycosylation does, however, increase stability against unfolding of the protein (15). Since S layers have shown a broad application potential in biotechnology, vaccine development, and molecular nanotechnology (for reviews, see references 23, 36, 38, and 42), a better understanding of the relevance of glycosylation of S-layer protein is of great importance.

ACKNOWLEDGMENTS

We thank Sonja Zayni and Elfriede Mayerhofer for excellent technical assistance.

This work was supported by the Österreichischer Fonds zur Förderung der wissenschaftlichen Forschung, project P8922-MOB, grant 4332 from the Jubiläumsfonds der Österreichischen Nationalbank (to P.M.), and the Österreichisches Bundesministerium für Wissenschaft und Forschung (to U.B.S.). The mass spectrometric work was supported by grant 4044 from the Jubiläumsfonds der Österreichischen Nationalbank (to G.A.).

REFERENCES

1. **Aduru, S., and B. T. Chait.** 1991. Californium-252 plasma desorption mass spectrometry of oligosaccharides and glycoconjugates: control of ionization and fragmentation. Anal. Chem. **63:**1621–1625.
2. **Augestad, I., and E. Berner.** 1954. Chromatographic separation of anomeric glycosides. II. New crystalline methylfuransides of galactose, arabinose and xylose. Acta Chem. Scand. **8:**251–256.
3. **Bax, A., and M. F. Summers.** 1986. ^{1}H and ^{13}C assignments from sensitivity-enhanced detection of heteronuclear multiple-bond connectivity by 2D multiple quantum NMR. J. Am. Chem. Soc. **108:**2093–2094.
4. **Berger, E., E. Buddecke, J. P. Kamerling, A. Kobata, J. C. Paulson, and J. F. G. Vliegenthart.** 1982. Structure, biosynthesis and function of glycoprotein glycans. Experientia **38:**1129–1162.
5. **Bock, K., J. F.-B. Guzman, and R. Norrestam.** 1988. Synthesis and conformational analysis of methyl 3-*O*-[α-L (and D)-rhamnopyranosyl]maltoside derivatives: a branched trisaccharide with the central glucopyranose residue in the $^{1}C_4$ conformation. Carbohydr. Res. **179:**97–124.
6. **Breitmaier, E., W. Voelter, G. Jung, and C. Tänzer.** 1971. Konfigurations-, Konformations- und Substitutionseinflüsse auf die ^{13}C-chemischen Verschiebungen von Glykosiden. Chem. Ber. **104:**1147–1154.
7. **Christian, R., P. Messner, C. Weiner, U. B. Sleytr, and G. Schulz.** 1988. Structure of a glycan from the surface-layer glycoprotein of *Clostridium thermohydrosulfuricum* strain L111-69. Carbohydr. Res. **176:**160–163.
8. **Dale, J. K., and C. S. Hudson.** 1930. Relations between rotary power and structure in the sugar group. XXX. The alpha and beta methyl-D-galactosides and their tetra-acetates. J. Am. Chem. Soc. **52:**2534–2537.
9. **Edge, A. B. S., C. R. Faltynek, L. Hof, L. E. Reichert, Jr., and P. Weber.** 1981. Deglycosylation of glycoproteins by trifluoromethanesulfonic acid. Anal. Biochem. **118:**131–137.
10. **Fischer, E., and L. Beensch.** 1896. Ueber die beiden optisch isomeren Methyl-Mannoside. Berichte **29:**2927–2931.
11. **Fischer, E., M. Bergmann, and A. Rabe.** 1920. Über Acetobromrhamnose und ihre Verwendung zur Synthese von Rhamnosiden. Berichte **53:**2362–2388.
12. **Gorin, P. A. J., and M. Mazurek.** 1975. Further studies on the assignment of signals in ^{13}C magnetic resonance spectra of aldoses and derived methyl glycosides. Can. J. Chem. **53:**1212–1223.
13. **Izumi, K.** 1987. Comparison of ^{13}C-spin-lattice relaxation times between sugars of the D-gluco- and D-galactopyranose series. Agric. Biol. Chem. **51:**1725–1726.
14. **Jansson, P.-E., L. Kenne, and H. Ottosson.** 1990. Synthesis of and nuclear magnetic resonance and conformational studies on some 1,2-linked disaccharide methyl glycosides containing D-mannose and L-rhamnose. J. Chem. Soc. Perkin Trans. **I:**2011–2018.
15. **Joao, H. C., I. G. Scragg, and R. A. Dwek.** 1992. Effects of glycosylation on protein conformation and amide proton exchange rates in RNase B. FEBS Lett. **307:**343–346.
16. **Klyne, W.** 1950. The configuration of the anomeric carbon atoms in some cardiac glycosides. Biochem. J. **47:**xli–xliii.
17. **Kochetkov, N. K., O. S. Chizhov, and A. S. Shashkov.** 1984. Dependence of ^{13}C chemical shifts on the spatial interaction of protons, and its application in structural and conformational studies of oligo- and polysaccharides. Carbohydr. Res. **133:**173–185.
18. **Lafitte, C., A. M. N. Phuoc Du, F. Winternitz, R. Wylde, and F. Pratveil-Sosa.** 1978. Synthesè et étude R. M. N. de disaccharide et trisaccharide dans la série du L-rhamnose. Carbohydr. Res. **67:**91–103.
19. **Lechner, J., and F. Wieland.** 1989. Structure and biosynthesis of prokaryotic glycoproteins. Annu. Rev. Biochem. **58:**173–194.
20. **Lipkind, G. M., N. E. Nifant'ev, A. S. Shashkov, and N. K. Kochetkov.** 1989. NMR and conformational study of branched oligosaccharides containing 2,3-disubstituted residues of α-L-rhamnose. Can. J. Chem. **68:**1238–1250.
21. **Lipták, A., Z. Szurmai, P. Nánási, and A. Neszmélyi.** 1982. Synthesis of 2-*O*-α-, 3-*O*-α-, 3-*O*-β-, and 4-*O*-α-L-rhamnopyranosyl-D-galactose. Carbohydr. Res. **99:**13–21.
22. **Lu, P. W., K. J. Kramer, P. A. Seib, D. D. Mueller, R. Ahmed, and T. L. Hopkins.** 1982. β-D-Glucopyranosyl-*O*-L-tyrosine: synthesis, properties and titre during insect development. Insect Biochem. **12:**377–381.
23. **Malcolm, A. J., P. Messner, U. B. Sleytr, R. H. Smith, and F. M. Unger.** 1993. Crystalline bacterial cell surface layers as combined carrier/adjuvants for conjugate vaccines, p. 195–207. *In* U. B. Sleytr, P. Messner, D. Pum, and M. Sára (ed.), Immobilised macromolecules: application potentials. Springer-Verlag, London.
24. **Mescher, M. F., and J. L. Strominger.** 1976. Purification and characterization of a prokaryotic glycoprotein from the cell envelope of *Halobacterium salinarium*. J. Biol. Chem. **251:**2005–2014.
25. **Messner, P., R. Christian, J. Kolbe, G. Schulz, and U. B. Sleytr.** 1992. Analysis of a novel linkage unit of O-linked carbohydrates from the crystalline surface layer glycoprotein of *Clostridium thermohydrosulfuricum* S102-70. J. Bacteriol. **174:**2236–2240.
26. **Messner, P., F. Hollaus, and U. B. Sleytr.** 1984. Paracrystalline cell wall surface layers of different *Bacillus stearothermophilus* strains. Int. J. Syst. Bacteriol. **34:**202–210.
27. **Messner, P., J. Kolbe, C. Schäffer, R. Christian, and U. B. Sleytr.** Glycoprotein nature of select bacterial S-layers. *In* T. J. Beveridge and S. F. Koval (ed.), Advances in bacterial crystalline surface layers. Plenum Publishing Corp., New York, in press.
28. **Messner, P., and U. B. Sleytr.** 1988. Separation and purification of S-layers from Gram-positive and Gram-negative bacteria, p. 97–104. *In* I. C. Hancock and I. R. Poxton (ed.), Bacterial cell surface techniques. John Wiley & Sons, Ltd., Chichester, United Kingdom.
29. **Messner, P., and U. B. Sleytr.** 1991. Bacterial surface layer glycoproteins. Glycobiology **1:**545–551.
30. **Messner, P., and U. B. Sleytr.** 1992. Crystalline bacterial cell-surface layers. Adv. Microb. Physiol. **33:**213–275.
31. **Montreuil, J.** 1984. Spatial conformation of glycans and glycoproteins. Biol. Cell **51:**115–131.
32. **Nielsen, P. F., K. Klarskov, P. Hojrup, and P. Roepsdorff.** 1988.

Optimization of sample preparation for plasma desorption mass spectrometry of peptides and proteins using nitrocellulose matrix. Biomed. Environ. Mass Spectrom. **17:**355–362.

33. **Peters, J., S. Rudolf, H. Oschkinat, R. Mengele, M. Sumper, J. Kellermann, F. Lottspeich, and W. Baumeister.** 1992. Evidence for tyrosine-linked glycosaminoglycan in a bacterial surface protein. Biol. Chem. Hoppe-Seyler **373:**171–176.
34. **Pfeffer, P. E., K. M. Valentine, and F. W. Parrish.** 1979. Deuterium-induced differential isotope shift ^{13}C NMR. 1. Resonance reassignments of mono- and disaccharides. J. Am. Chem. Soc. **101:**1265–1274.
35. **Pozsgay, V., J.-R. Brisson, and H. J. Jennings.** 1987. Synthetic oligosaccharides related to group B streptococcal polysaccharides. The rhamnotriose moiety of the common antigen. Can. J. Chem. **65:**2764–2769.
36. **Pum, D., M. Sára, P. Messner, and U. B. Sleytr.** 1991. Two-dimensional (glyco)protein crystals as patterning elements for the controlled immobilisation of functional molecules. Nanotechnology **2:**196–202.
37. **Ritchie, R. G. S., N. Cyr, B. Korsch, H. J. Koch, and A. S. Perlin.** 1975. Carbon-13 chemical shifts of furanosides and cyclopentanol. Configurational and conformational influences. Can. J. Chem. **53:**1424–1433.
38. **Sára, M., S. Küpcü, C. Weiner, S. Weigert, and U. B. Sleytr.** 1993. Crystalline protein layers as isoporous molecular sieves and immobilisation and affinity matrices, p. 71–86. *In* U. B. Sleytr, P. Messner, D. Pum, and M. Sára (ed.), Immobilised macromolecules: application potentials. Springer-Verlag, London.
39. **Shashkov, A. S., G. M. Lipkind, Y. A. Knirel, and N. K. Kochetkov.** 1988. Stereochemical factors determining the effects of glycosylation on the ^{13}C chemical shifts in carbohydrates. Magn. Reson. Chem. **26:**735–747.
40. **Sleytr, U. B., and P. Messner.** 1983. Crystalline surface layers on bacteria. Annu. Rev. Microbiol. **37:**311–339.
41. **Sleytr, U. B., and P. Messner.** 1988. Crystalline surface layers in procaryotes. J. Bacteriol. **170:**2891–2897.
42. **Sleytr, U. B., D. Pum, M. Sára, and P. Messner.** 1992. Two-dimensional protein crystals as patterning elements in molecular nanotechnology, p. 167–177. *In* A. Aviram (ed.), Molecular electronics—science and technology. AIP Conference Proceedings 262. American Institute of Physics, New York.
43. **Stevens, J. D., and H. G. Fletcher, Jr.** 1968. The proton magnetic resonance spectra of pentafuranose derivatives. J. Org. Chem. **33:**1799–1805.
44. **Suprenant, H. L., J. E. Sarneski, R. R. Key, J. T. Byrd, and C. N. Reilley.** 1980. Carbon-13 NMR studies of amino acids: chemical shifts, protonation shifts, microscopic protonation behavior. J. Magn. Reson. **40:**231–243.
45. **Windholz, M. (ed.).** 1983. The Merck index, 10th ed., p. 1406. Merck & Co., Inc., Rahway, N.J.